Frontiers in Ecology and the Environment

Geomorphic controls on salmon nesting patterns described by a new, narrow-beam terrestrial–aquatic lidar

Jim A McKean, Dan J Isaak, and Charles W Wright

Front Ecol Environ 2008; 6, doi:10.1890/070109

Geomorphic controls on salmon nesting patterns described by a new, narrow-beam terrestrial–aquatic lidar

Jim A McKean[1*], Dan J Isaak[2], and Charles W Wright[3]

Riverine aquatic biodiversity is rapidly being lost worldwide, but preservation efforts are hampered, in part because studies of these dynamic environments are limited by cost and logistics to small local surveys. Full understanding of stream ecosystems requires precise, high-resolution mapping of entire stream networks and adjacent landforms. We use a narrow-beam, water-penetrating, green lidar system to continuously map 10 km of a mountain stream channel, including its floodplain topography, and wavelet analyses to investigate spatial patterns of channel morphology and salmon spawning. Results suggest the broadest fluvial domains are a legacy of approximately 15 000 years of post-glacial valley evolution and that local pool–riffle channel topography is controlled by contemporary hydraulics operating on this broad template. Salmon spawning patterns closely reflect these hierarchical physical domains, demonstrating how geomorphic history can influence modern distributions of aquatic habitat and organisms. The new terrestrial–aquatic lidar could catalyze rapid advances in understanding, managing, and monitoring of valuable aquatic ecosystems through unprecedented mapping and attendant analyses.

Front Ecol Environ 2008; 6, doi:10.1890/070109

Streams are one of the most dynamic components of landscapes and their modern morphology represents not only a response to contemporary sediment and water supplies, but also reflects a legacy of past environmental conditions. The result is a patchy mosaic of physical habitats that structure stream biota at multiple spatial scales (Frissell *et al.* 1986; Fausch *et al.* 2002). Disentangling these multiscale relationships is difficult, but fundamental to understanding and effectively managing ecological systems (Levin 1992). Currently, cost and logistics limit detailed stream studies to small spatial extents, making it difficult to analyze interactions among larger channel domains or to extrapolate to the scale of stream networks. There has been some progress in using remote-sensing techniques to map stream physical characteristics over large or restricted areas (Mertes 2002), but older airborne sensors are limited by their inability to penetrate water and directly measure submerged channel topography at high resolution and with no local field calibration.

We used a new lidar system, NASA's Experimental Advanced Airborne Research Lidar (EAARL), to continuously map three-dimensional channel and floodplain topography in streams that provide spawning habitat of a federally listed (threatened) population of Chinook salmon (*Oncorhynchus tschawytscha*). The EAARL sensor is a full waveform, green-wavelength lidar whose low beam divergence and moderate pulse repetition rate enable continuous, high-resolution mapping of submerged channel topography, floodplain topography, and vegetation in one integrated dataset (Wright and Brock 2002; Brock *et al.* 2004; Nayegandhi *et al.* 2006; WebTable 1). We explored linkages between modern channel topography and the evolution of floodplain geomorphology in the ~15 000 years since the last major glaciation. We then quantitatively investigated how channel features structure the distribution of salmon spawning at multiple spatial scales. We limited our analysis to patterns of topographic variability in the channel bed, as Chinook salmon prefer spawning on convex-upward channel-bed components, which are generally transitional areas (riffles) between pools (Bjornn and Reiser 1991). We hypothesized that spatial patterns of spawning would correlate with the distribution and amplitude of these local convex-upward segments of the channel bed. However, we were also interested in patterns of co-occurrence between spawning and channel-bed topography over broader scales, where erosion and sediment deposition over the past ~15 000 years might have produced larger, distinct geomorphic domains within an unconfined alluviated valley.

Field area and methods

EAARL data were acquired over ~200 km of streams in low-flow conditions with high water clarity during 5 hours of flight-time in October of 2004. The lidar data were interpolated to produce digital elevation models (DEMs) with 3-m grid spacing. The subset of our mapped stream network selected for detailed study consisted of

[1]*US Forest Service, Rocky Mountain Research Station, Boise, ID 83702 (jmckean@fs.fed.us); [2]US Forest Service, Rocky Mountain Research Station, Boise, ID 83702; [3]NASA Goddard Space Flight Center, Wallops Flight Facility, Wallops Island, VA 23337*

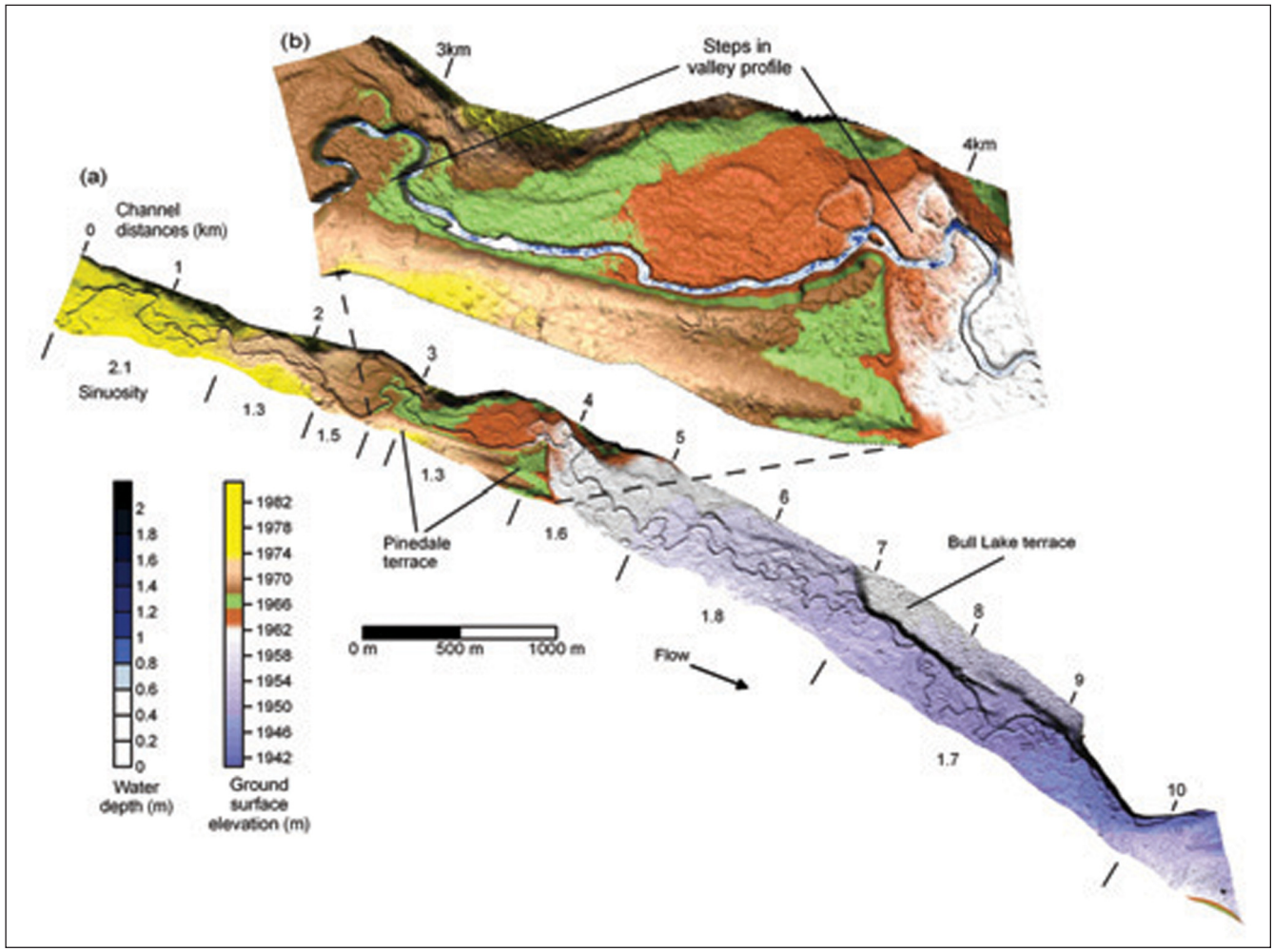

Figure 1. *(a) Digital elevation model of upper Bear Valley Creek. Reference distances are measured along the channel and sinuosity is calculated as channel length/straight-line valley distance over the indicated valley segments. (b) Inset showing degraded step in the valley profile at distance ~3800 m and shorter valley step at ~2800 m. For higher resolution, see WebFigure 3.*

10 km of meandering pool–riffle channel (sensu Montgomery and Buffington 1997) in Idaho's Bear Valley Creek, a tributary stream in the upper Middle Fork Salmon River drainage. Bear Valley Creek is a gravel-bed stream that flows through a broad, gentle valley, partially bounded by remnants of two glacial terraces from Bull Lake- (~140 000 years before present [ybp]) and Pinedale- (~22 000 ybp) age glaciations (Schmidt and Mackin 1970; Figure 1). The study channel was 10–15 m wide, 0.1–2 m deep, with longitudinal gradients of 0.17–0.61% calculated over 200-m reach lengths, and had a median substrate size of ~50 mm. Data describing salmon nest distributions were obtained by annual surveys of the study reach from 1995–2005. We used this aggregation to improve sample size because annual salmon abundances were well below historic levels.

We investigated spatial structure in channel-bed topography and spawning patterns using one-dimensional, continuous wavelet transforms. We characterized the bed topography by the elevation profile along the thalweg (the line connecting the deepest points as one moves down the channel). The thalweg was hand digitized in the EAARL data. The wavelet technique analyzes spatial or temporal patterns in the frequency domain by comparing pieces of a continuous signal (in our case, the elevation profile down the channel thalweg or the spatial distribution of salmon nests down the channel) to a reference waveform and calculating transform coefficients that describe the similarity of any portion of the original signal to the reference wavelet (Mallat 1989; Daubechies 1992; Hubbard 1998; Torrence and Compo 1998). We used an eighth-order Gaussian and a biorthogonal 1.5 reference wavelet, respectively, for the channel-bed topography and spawning data (WebFigure 1 a, b). The Gaussian wavelet has a smoothly varying form, similar to channel-bed profiles and, when centered on a channel profile convexity, the wavelet coefficients were positive; when the wavelet was out of phase and centered on a pool or concavity, the coefficients were negative. The magnitude of coefficients was proportional to the vertical amplitude of the bed elevation changes. The biorthogonal wavelet varied more abruptly and was therefore appropriate for a nearly binomial variable, such as presence/absence of fish nests. A variety of other refer-

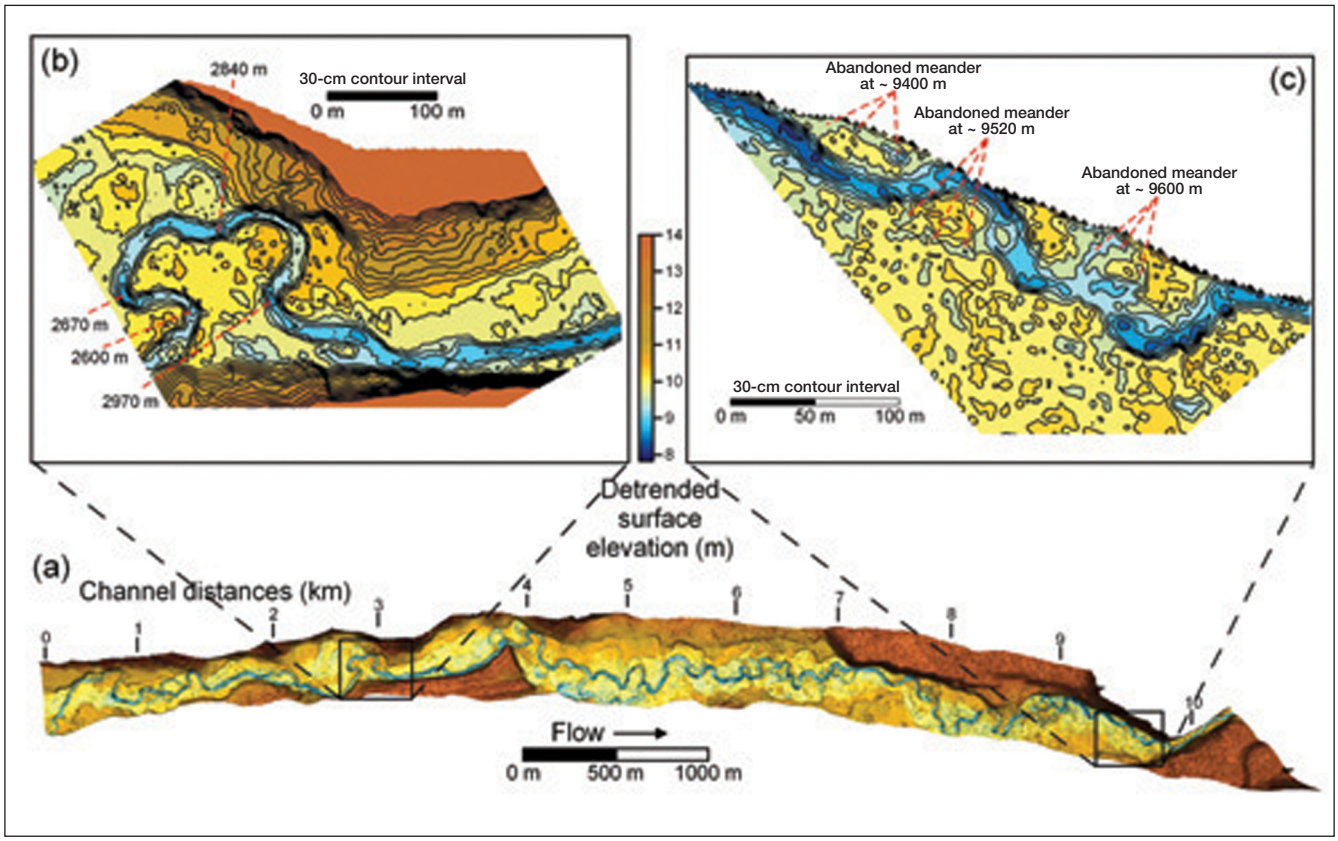

Figure 2. *(a) Channel, floodplain, and terrace topography after the valley gradient has been removed. (b and c) Contour maps of selected channel reaches, showing the ability of EAARL to simultaneously resolve floodplain, terrace, and channel topography. All digital topography produced from EAARL data gridded to a 3-m interval. For higher resolution, see WebFigure 4*

ence wavelets were investigated for both channel and spawning data and several worked nearly as well as the Gaussian and biorthogonal wavelet. Wavelet transforms are particularly powerful because the analysis can rapidly explore spatial scaling of patterns, simply by changing the length of the reference wavelet, while keeping its form constant, and repeating the transform.

Results

The EAARL data revealed two major domains of channel morphology and aquatic habitat, separated by a narrow, degraded step in the valley profile at a channel distance of ~3800 m (Figure 1 a, b). The step is about 3 m tall and marks the transition from an upstream, generally straight channel, with extensive plane-bed reaches (Montgomery and Buffington 1997) to a downstream, strongly meandering pool–riffle channel. A similar, but shorter and steeper step in the valley profile also occurs at a large, irregular channel meander from 2600 to 2970 m (Figure 1b). In Figure 2, the general valley gradient has been removed from the same data ("detrending" the topography), to emphasize subtle erosion surfaces inset between the two major glacial terraces and the details of channel erosion of the valley fill. Numerous abandoned channels and smaller side channels are visible in the floodplain; many of these are quite subtle, with depths of only 20–50 cm. Figures 2b and 2c are contour maps of short reaches that illustrate the channel topographic detail distinguished by EAARL. The three-dimensional morphology of individual pools and riffles in the main channel is easily mapped (eg see pools at channel distances of ~2600 m, ~2670 m, ~ 2840 m, and ~2970 m; Figure 2b). Abandoned meanders are mapped in Figure 2c at channel distances of ~9400 m, ~9520 m, and ~9600 m. These old meanders reconnect to the main channel at high flows and are typical of off-channel aquatic habitat in this portion of the valley.

Figure 3a shows the distribution of salmon nests from 1995 to 2005. The channel topography appears to have been very constant over this period; Figure 3b shows the channel-bed elevation profile analyzed by the Gaussian wavelet. In Figure 3b, the valley gradient has been removed to better illustrate local channel topographic details, but the wavelet transform was computed on the original data that includes the valley gradient.

Initially, we calculated Gaussian wavelet coefficients for the channel profile across all spatial scales from 1 to 750 m (see all coefficients plotted as a function of scale and position in WebFigure 2). Visual examination and trial transects through WebFigure 2 suggested distinctive channel profile patterns at several spatial scales: 600 m, 310 m, and 95 m (Figure 3 c,d,e). The spawning site distribution was then analyzed at the same scales for com-

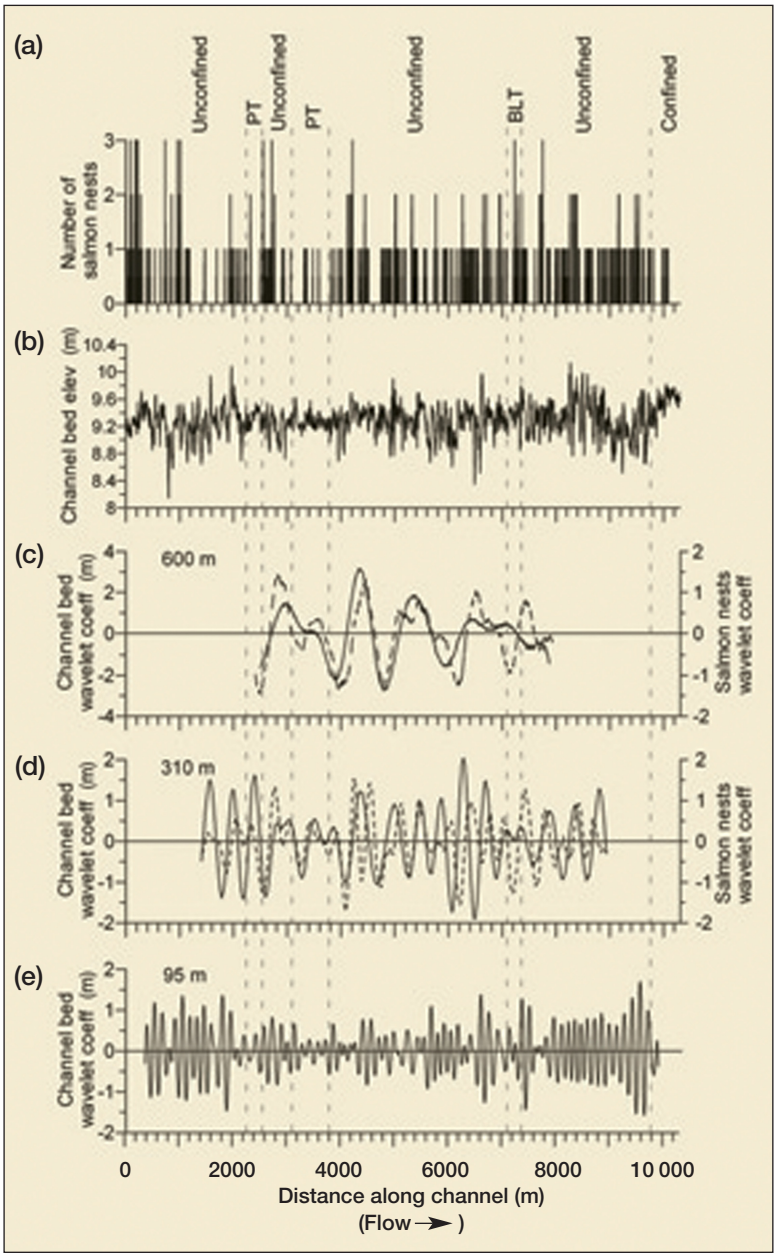

Figure 3. *Wavelet analyses of channel topography and salmon nests. Local domains of channel morphology and aquatic habitat are separated by vertical dashed lines: PT = channel semi-confined by Pinedale-age terrace, BLT = channel semi-confined by Bull Lake-age terrace. (a) Distribution of salmon nests during 1995–2005. (b) Detrended channel elevation profile mapped along the line connecting the deepest points in the channel. (c, d, e) Continuous wavelet transforms of channel-bed topography (Gaussian – solid line) and salmon nests (biorthogonal – dashed line) using reference wavelets of 600 m, 310 m, and 95 m, respectively. These plots are horizontal transects through the data in WebFigure 2 at the three respective scales.*

parison. Wavelet transforms at a 600-m scale detected large geomorphic domains in the valley, although not with great precision, because of the coarse scale of analysis (Figure 3c). The upstream and downstream limits of the plane-bed channel reach shown in Figure 1b are mapped in Figure 3c by the positive and negative peaks of channel coefficients at distances 3000 m and 4000 m, respectively. The channel coefficients are small in the plane-bed section between these peaks. Further downstream, the analysis maps broad undulations in the vertical profile of the unconfined channel that decline in vertical amplitude with distance downstream, away from the step in the valley profile at channel distance 3800 m. The cause of these long, low frequency waves in the bed elevation profile are under investigation, but may be related to a locally high sediment supply, where the channel is eroding laterally into the Pinedale-age terrace between distances of ~3000–3800 m and where the channel bed is eroding as it descends the step in the valley profile from 3800–4000 m. The pattern of salmon nest coefficients mirrors these broad channel characteristics along most of the profile.

At an intermediate spatial scale of 310 m, the wavelet analysis detected the combined effects of the broad geomorphic domains and local hydraulics on channel topography (Figure 3d). The regular pattern of major negative peaks generally corresponds closely to a series of the deepest pools in the channel, consistently spaced at ~400 m intervals. Two interruptions occur at channel distances of ~2700–4000 m and ~7000–7400 m, where the channel is located against large glacial terraces, the stream is straighter, and the channel bed is smooth. The pattern of salmon nests still closely follows that of channel elevations, although peaks in nest coefficients are often offset ~50–100 m downstream from the centers of clusters mapped in Figure 3a because of the lateral asymmetry of the biorthogonal reference wavelet (WebFigure 1b).

In Figure 3e, the analysis at a 95-m scale faithfully maps nearly all individual pools and riffles through the 10-km stream length. For example, the four small pools and intervening riffles in the large meander in Figure 2b are each correctly mapped in Figure 3e. The spacing and amplitude of variations in bed elevation also change dramatically over the study reach, with larger and more frequent pools and riffles concentrated upstream of 2000 m and downstream of 5600 m. Straight plane-bed reaches adjacent to glacial terraces are also mapped with good spatial resolution (eg coefficients near zero between ~2200–2500 m and ~3200–3800m; Figure 3e). At this scale, imprecision of nest geolocations made it impossible to correlate nests and channel data.

Discussion

Wavelet analyses are an efficient technique to explore spatial scaling of habitat mapped by EAARL. These analyses revealed hierarchical scales of channel morphol-

ogy and salmon spawning that result from a combination of environmental legacies and modern hydraulics. The steps in the valley profile that bound broad geomorphic domains apparently represent upstream limits of episodic valley erosion that occurred when the sediment supply declined after the last glacial maximum and the stream began to remove the deposited glacial outwash debris and re-grade the valley to lower levels, in a process that is still ongoing. The large glacial terrace remnants and straight plane-bed channel reaches along portions of the valley margin are an important geomorphic setting that eliminates spawning habitat in ~15% of the length of upper Bear Valley Creek. Where unconfined by terraces, the channel meanders widely and develops the classic alternating pool–riffle morphology preferred by spawning salmon. Within this domain, contemporary open-channel hydraulics control medium- to fine-scale channel morphology and habitat structure. The deepest pools form at major meanders, and these larger local incisions create undulations in the general stream longitudinal profile over ~300–400-m distances. Smaller pools and riffles, also driven by local hydraulics, occur between the major pools, particularly in the downstream half of the study reach, where the valley gradient is lower. Salmon nest distributions generally agree with patterns in channel topography, with the majority of spawning occurring in the unconfined valley reaches downstream of distance ~5500 m or upstream of distance 1200 m, implying that, as expected, bedforms are a primary control on spawning sites in Bear Valley Creek.

This project demonstrates one of many potential applications of EAARL technology. Another is stream monitoring, for which resource agencies annually spend millions of dollars to support field crews that employ a variety of surveying techniques. For instance, an extensive channel monitoring program in the Columbia River Basin has an annual budget of about $1 500 000 (Henderson *et al.* 2005). The unique, georeferenced EAARL maps of channel morphology could dramatically increase the objectivity and cost-effectiveness of this work. Changing local conditions, different scales of study, and EAARL's experimental status make it difficult to directly compare costs of traditional and EAARL stream surveys. In our study area, a field survey of 200 m of channel topography costs ~$2000 or $10 000 km^{-1}, although it would have been extremely tedious to extend the survey to one kilometer. Acquisition of EAARL data for 200 stream km in the same year costs $20 000 (~$100 km^{-1}), which includes mobilization of the instrument from the east coast of the US to Idaho. A trained technician can process a kilometer of raw EAARL data to produce a "clean", bare-earth DEM in about one week, depending on the complexity of the near-channel topography and vegetation. However, more important than a large per-unit-channel-length cost advantage is the opportunity to continuously map, rather than locally sample, a whole stream network. Even intensive monitoring programs typically only resurvey sites every 5 years, thus requiring >10 years to assess changing trends. The economics of EAARL surveys will allow more frequent monitoring to rapidly detect changes in the physical attributes of channels.

Wavelet transforms are also an objective, quantitative measure of the quality of habitat, and sequential wavelet transforms of multi-temporal EAARL data could provide a robust gauge of environmental change. The EAARL data can also define boundary conditions necessary to support predictions based on computational fluid-dynamics models about many important channel characteristics, such as local water velocity, patterns of bed shear stress and mobility, and, possibly, median grain size on the bed. Individual-based biological models of fish survival and growth are supported by these same channel boundary conditions and relationships between flow velocity, macroinvertebrate drift, and foraging efficiency. The same topographic data also constitute the basis for design of engineered stream restorations, another activity with annual expenditures of millions of dollars in the US alone. Correlative biological models could also benefit from more precisely measured predictor variables and the ability to derive new habitat measures that account for spatial context, scaling relationships, or habitat complementation (Dunning *et al.* 1992). To facilitate several of these applications, we are developing a GIS-based toolkit to automatically extract from EAARL data standard metrics that are routinely used by aquatic scientists to describe streams (eg channel longitudinal gradient, sinuosity, and cross-sectional characteristics). The toolkit will include algorithms to remove the general valley gradient from channel data and produce maps such as that seen in Figure 2a.

Because streams integrate the terrestrial and aquatic complexities of their watersheds, tools that seamlessly map both domains are required to fully understand these systems. The EAARL instrument is a new breed of sensor that provides accurate, high-resolution, continuous sub-aerial and sub-aqueous data that support integrated analyses of channel, floodplain, and riparian ecosystems at scales spanning short reaches to whole stream networks. We are on the threshold of a new era of mapping and monitoring channel physical conditions, one in which piecemeal local sampling may be replaced or complemented by nearly complete inventories of stream networks.

Acknowledgements

This research was supported by the USDA Forest Service, Rocky Mountain Research Station, NASA Goddard Space Flight Center, and NOAA Northwest Fishery Science Center. We thank R Thurow, USDA Forest Service, for data on salmon spawning distributions.

References

Bjornn TC and Reiser DW 1991. Habitat requirements of salmonids in streams. In: Meehan WR (Ed). Influences of forest and rangeland management on salmonid fishes and their habitats. Bethesda, MD: American Fisheries Society.

Brock JC, Wright CW, Clayton TD, and Nayegandhi A. 2004. Lidar optical rugosity of coral reefs in Biscayne National Park, Florida. *Coral Reefs* **23**: 48–59.

Daubechies I. 1992. Ten lectures on wavelets. Philadelphia, PA: Society for Industrial Applied Mathematics.

Dunning JB, Danielson BJ, and Pulliam HR. 1992. Ecological processes that affect populations in complex landscapes. *Oikos* **65**: 169–75.

Fausch KD, Torgersen CE, Baxter CV, and Li HW. 2002. Landscapes to riverscapes: bridging the gap between research and conservation of stream fishes. *BioScience* **52**: 483–98.

Frissell CA, Liss WJ, Warren CE, and Hurley MD. 1986. A hierarchical framework for stream habitat classification: viewing streams in a watershed context. *Environ Manage* **10**: 199–214.

Henderson RC, Archer EK, Bouwes BA, *et al.* 2005. PACFISH/INFISH Biological Opinion (PIBO): effectiveness monitoring program seven-year status report 1998 through 2004. Fort Collins, CO: US Forest Service, Rocky Mountain Research Station. General Technical Report RMRS-GTR-162.

Hubbard BB. 1998. The world according to wavelets, 2nd edn. Natick, MA: AK Peters Ltd.

Levin SA. 1992. The problem of pattern and scale in ecology. *Ecology* **73**: 1943–67.

Mallat SF. 1989. A theory for multiresolution signal decomposition: the wavelet representation. *IEEE T Pattern Anal* **11**: 674–93.

Mertes LAK. 2002. Remote sensing of riverine landscapes. *Freshwater Biol* **47**: 799–816.

Montgomery DR and Buffington JM. 1997. Channel-reach morphology in mountain drainage basins. *Bull Geol Soc Am* **109**: 596–611.

Nayegandhi A, Brock JC, Wright CW, and O'Connell MJ. 2006. Evaluating a small footprint, waveform-resolving lidar over coastal vegetation communities. *Photogramm Eng Rem S* **72**: 1407–17.

Schmidt DL and Mackin JH. 1970. Quaternary geology of Long and Bear Valleys, west–central Idaho. Washington, DC: US Government Printing Office.

Torrence C and Compo GP. 1998. A practical guide to wavelet analysis. *B Am Meteorol Soc* **79**: 61–78.

Wright W and Brock J. 2002. A lidar for mapping shallow coral reefs and other coastal environments. In: Proceedings of the 7th International Conference on Remote Sensing for Marine and Coastal Environments; 2002 May 20–22; Miami, FL. Ann Arbor, MI: Environmental Research Institute of Michigan.

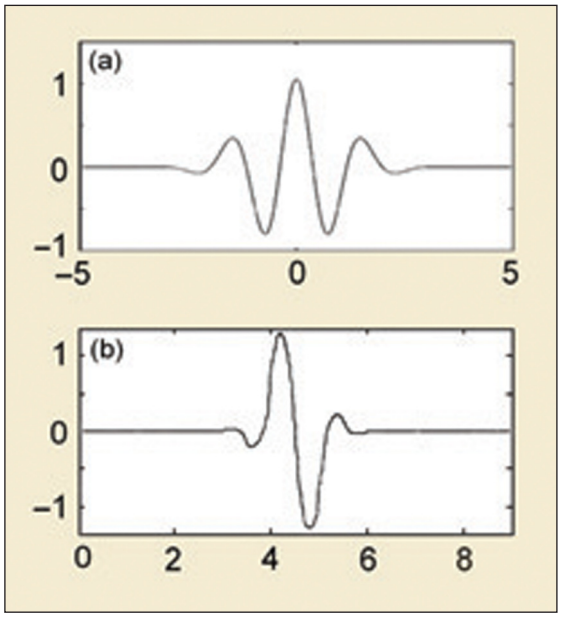

WebFigure 1. *(a) Gaussian eighth-order reference wavelet. (b) Biorthogonal 1.5 reference wavelet.*

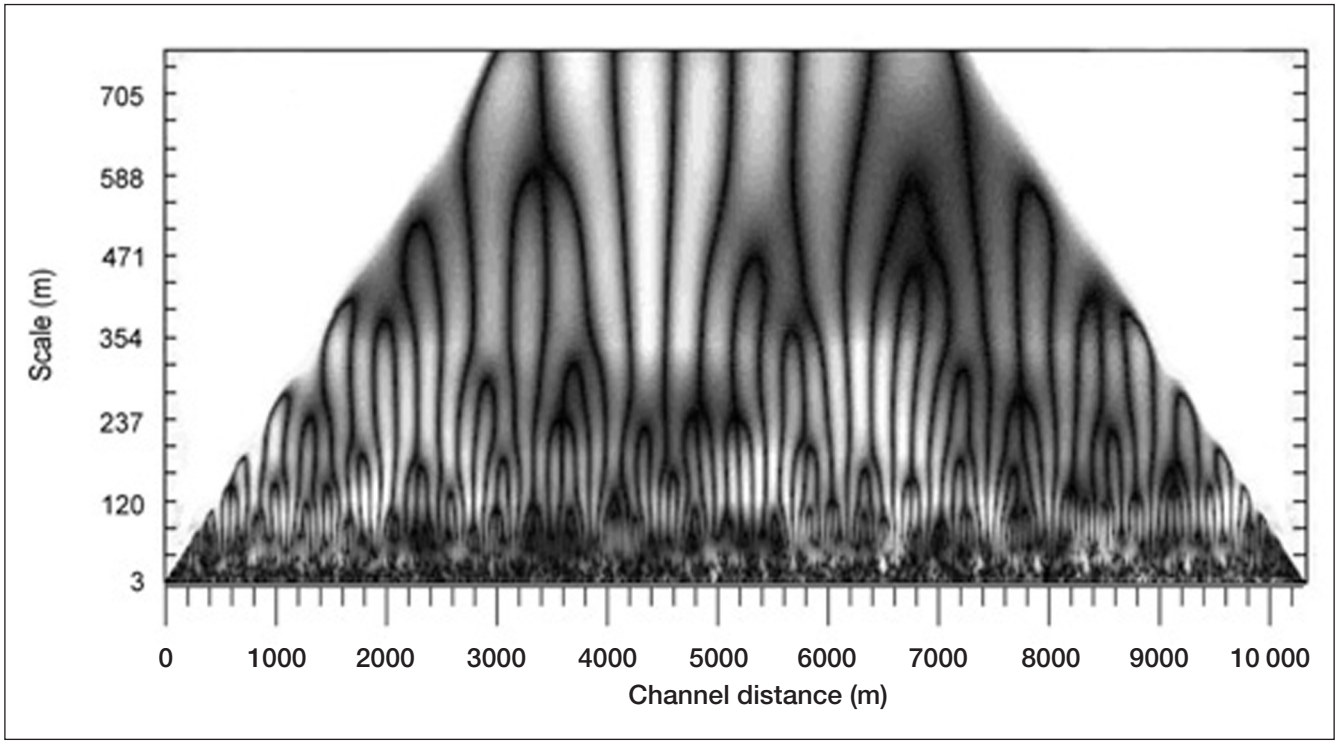

WebFigure 2. *Gray-scale plot of Gaussian (eighth-order) wavelet transform coefficients of channel thalweg. Darker tones are coefficients near zero and lighter tones are strongly positive or negative coefficients. Scale defines the length of the reference wavelet (ie the spatial scale of elements of the channel profile compared to the reference wavelet). Edge effects occur further into the data as the spatial scale of analysis increases.*

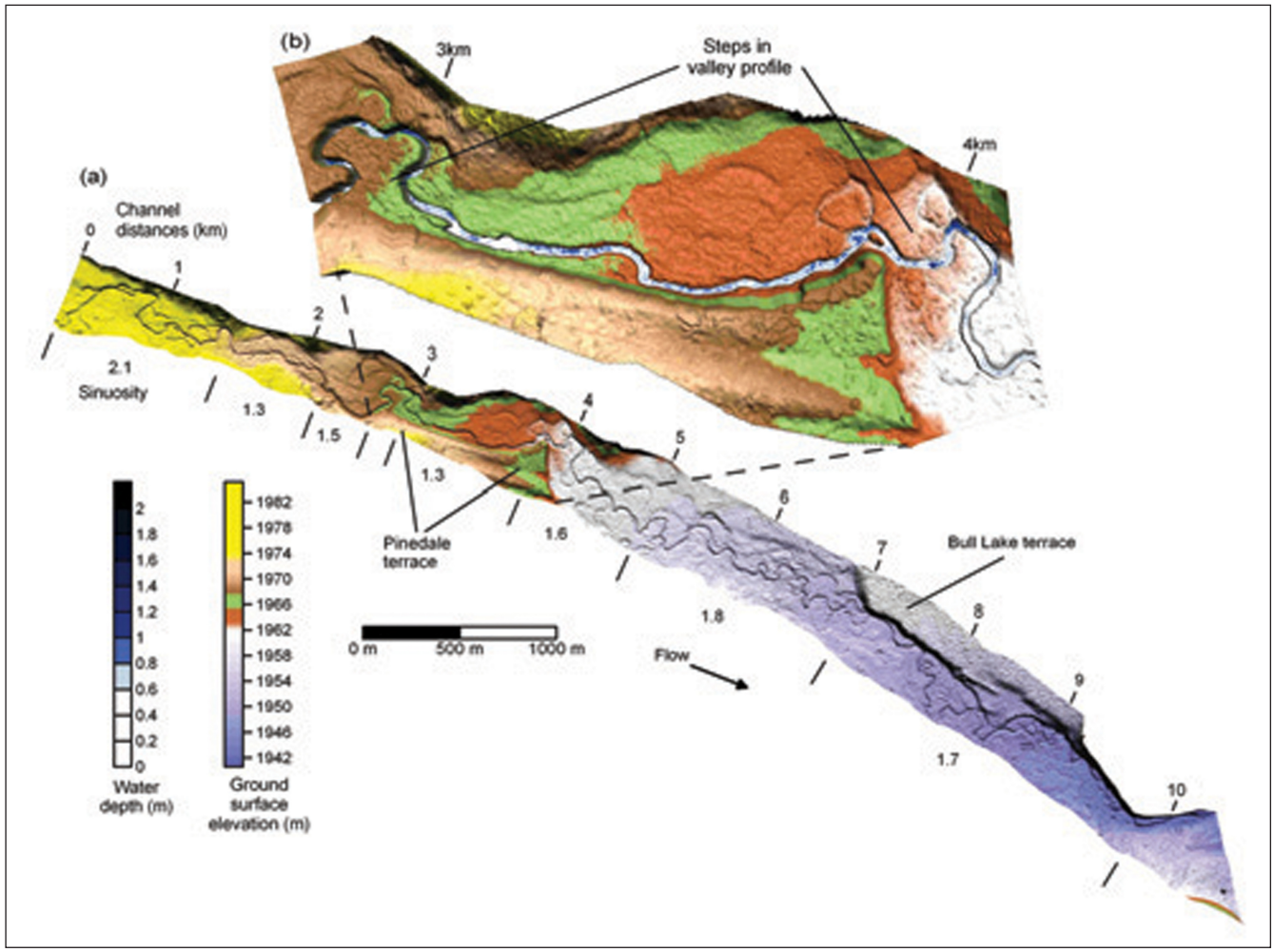

WebFigure 3. *Higher-resolution view of Figure 1. (a) Digital elevation model of upper Bear Valley Creek. Reference distances are measured along the channel and sinuosity is calculated as channel length/straight-line valley distance over the indicated valley segments. (b) Inset showing degraded step in the valley profile at distance ~ 3800 m and shorter valley step at ~ 2800 m.*

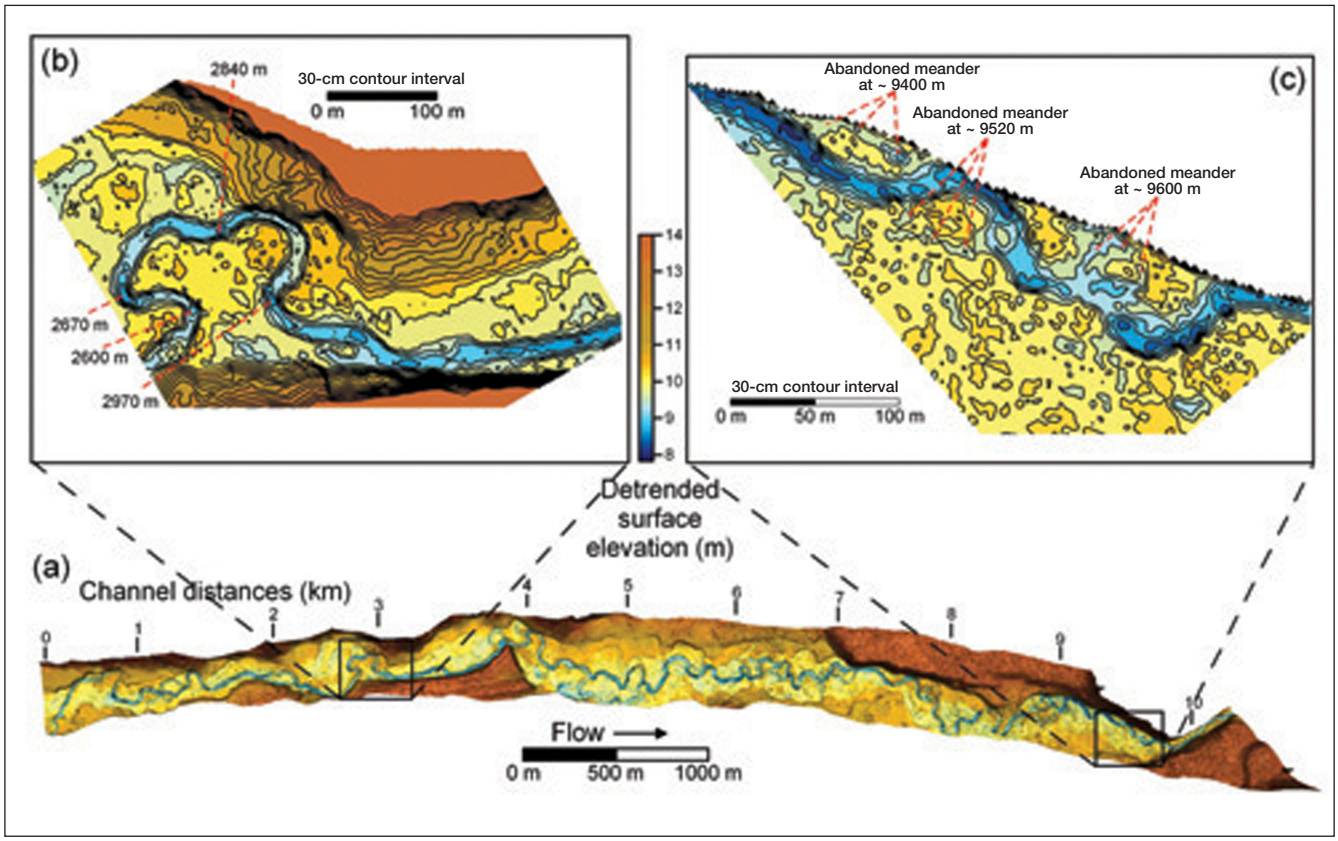

WebFigure 4. *Higher resolution view of Figure 2. (a) Channel, floodplain, and terrace topography after the valley gradient has been removed. (b and c) Contour maps of selected channel reaches, showing the ability of EAARL to simultaneously resolve floodplain, terrace, and channel topography. All digital topography produced from EAARL data gridded to a 3-m interval.*

WebTable 1. EAARL specifications

Survey altitude	300 m (AGL)
Survey flight speed	50 m s^{-1}
Laser	Neodymium-doped Yttrium Aluminum Garnet (Nd:YAG)
Laser wavelength	532 nm
Laser pulse energy	70 μJ $pulse^{-1}$ (eye safe)
Laser pulse length	1.2 ns
Laser spot diameter from 300 m AGL	20 cm
Laser pulse frequency	3–10 kHz
Raster scan rate	25 s^{-1}
Digitized waveform samples per laser pulse	16384
Digitizer temporal resolution	1 ns (14.9 cm in air, 11.3 cm in water)
Data swath width from 300 m AGL	240 m
Single pass sample spacing	2 m x 2 m at swath center
Vertical accuracy	~10 cm RMSE
Horizontal accuracy	~50 cm RMSE
Operation water depths	0–25 m (clarity dependent)
Other integrated sensors	RGB video; high resolution CIR digital camera
Processing software	Airborne Laser Processing Software (ALPS)

